Available online at www.sciencedirect.com
ScienceDirect
Journal of Sound and Vibration 310 (2008) 947–965
JOURNAL OF SOUND AND VIBRATION
www.elsevier.com/locate/jsvi

Optimal position and shape of applied damping material

Magnus Alvelid[a,b,*]

[a]Trelleborg Rubore AB, SE-39128 Kalmar, Sweden
[b]Department of Applied Mechanics, Chalmers University of Technology, SE-41296 Göteborg, Sweden

Received 21 December 2006; received in revised form 8 August 2007; accepted 15 August 2007
Available online 18 October 2007

Abstract

The frequency averaged transverse vibration levels of a plate with a harmonic excitation is minimized by optimizing the position and shape of attached passive constrained layer damping. A modified gradient method is used in the finite-element context to successively add pieces of constrained damping layers at the elemental positions showing the steepest gradient of the goal function as a result of the treatment. The coding is done in MATLAB and different stop conditions can be included so as to set limits for the cost or weight that can be spent on the treatment of the structure. It is demonstrated that for a square plate, only a few iterations are needed to reduce the average vibration level with up to 18 dB by covering less than 30 percent of the surface with a sandwich type applied damping material. For an industrial example, measurements show that the solution proposed by the optimization procedure will decrease the vibration levels for the two dominant modes of vibrations with 3–4 dB, by covering 3.4 percent of the surface with a single-sided constraining layer type applied damping material.

1. Introduction

Passive constrained layer damping (PCLD) is today a common method for reducing vibrations in vehicles, e.g., cars. Especially, when it comes to brake systems, the use of PCLD is widely spread and almost all cars manufactured today have a "shim" mounted between the backing plate of the brake pad and the brake piston. The shim consists of a thin damping layer attached to a thin metal plate. Also for engine applications, the use of applied damping material (ADM) has become more and more common in order to reduce vibrations and sound radiation arising from local deformation modes of engine components like oil pans, front covers, valve covers, air intake manifolds, etc.

Constrained layer damping (CLD) is a very efficient technology in terms of reducing vibration energy. The technical principle is that of a high loss factor viscoelastic layer (e.g., rubber) attached to the base structure and constrained on its other side by a stiff layer (e.g., metal). Thus, when the base structure vibrates in bending the viscoelastic layer will be subjected to a large shear deformation resulting in conversion of kinetic energy into heat. An overview of the procedures for the modelling and analysis of thin-rubber layers is given by

*Corresponding author at: Department of Applied Mechanics, Chalmers University of Technology, SE-41296 Göteborg, Sweden. Tel.: +46 708 698903.
E-mail address: magnus.alvelid@telia.com

0022-460X/$ - see front matter © 2007 Elsevier Ltd. All rights reserved.
doi:10.1016/j.jsv.2007.08.024

Alvelid and Enelund in Ref. [1]. Given an existing finite-element mesh for the base structure, it is of large interest to know where to add ADM in order to get the most reduction possible in terms of vibration energy of the system, given a limited amount of added on material. Normally, this ''optimization'' is done manually by studying the deformed shape of the structure at a certain frequency which represents a vibration level peak. Then ADM is added on the structure in the finite-element (FE) model and a second computer run is made in order to give comparable result. If necessary more iterations are made. However, this procedure can only give a rough estimate of an optimal use of the ADM material in terms of weight, cost and placement and therefore a more exact and automated process is sought for. The complementary optimization problem where the build up of the different layers in a sandwich material is optimized in order to reduce vibration levels, is not within the scope of this article. The reason is twofold: first, such optimization procedures are already commercially available using finite-element modelling technique, and second, the most common problem for the design engineer is that applied damping materials are only industrially available in a limited number of versions and hence the main problem is to determine the shape of the ADM with a given material specification, since there is a limited option to vary the individual thicknesses of the layers.

Optimization is a wide field of research. Within the area of noise and vibrations, the early 1990s is a period which represents a large interest in the possibilities to optimize secondary sources in active noise control systems in order to mitigate noise and vibrations problems in, e.g., aircraft, automotive and space applications. Among the significant contributions to the knowledge within this engineering field, we acknowledge the pioneering work by Nelson and Elliott which resulted in the textbook ''Active control of sound'' [2]. Alvelid [3] demonstrated how the simulation of secondary sources in a finite-element model resulted in a quadratic optimization problem that could be solved directly by taking the derivative of the goal function with respect to the secondary source strength vector and then solving the resulting linear system of equations. Today, however, the two dominant approaches discussed in literature to solve optimization problems are the ''gradient based'' approach and the ''genetic'' approach—or wider, the ''evolutionary approach''. The gradient-based approach is simple and efficient in feed-back loops where the control algorithm calculates the change of the error or the goal function with respect to the design variables from one iteration to the other and then moves in the direction of the steepest descent, see e.g., Ref. [4]. An introduction to the gradient-based approach is given in Ref. [5] where the optimal placement of loudspeakers in an active noise control system is analyzed, using the same approach as in Ref. [3] for calculating the optimal source strengths for each loudspeaker configuration. Later, Moshrefi-Torbati et al. [6], have analyzed the design optimization of a satellite boom structure with respect to vibrations in a chosen frequency spectra. The frequency-averaged response in terms of the sum of the square of the velocities in each joint of the satellite boom, is used as a goal function. The choice of goal function is of the same kind as in the present article. Within the engineering field of CLD, Liu and Wang [7] have studied the integration of enhanced active constrained layer and active-passive hybrid constrained layer treatments using a mixed method where a genetic method called differential evolution (DE) for continuous function optimization is combined with the gradient based method sequential quadratic programming (SQL). The authors found that convergence towards a global optimum was much approved by using the output from the DE procedure as an input to the SQL scheme. The physical model did only cover in-plane displacements and strains, however, and no transverse displacements. Zheng et al. [8] have studied the optimal extent and placement of PCLD on beams. The beams were modelled using Euler–Bernoulli theory and the boundary conditions were of the type of simply supported. The dynamic problem was solved by expanding the displacement fields into a series of assumed modes and then applying Hamilton's principle to create a linear system of equations with the generalized co-ordinates as unknowns. The linear system of equations was solved numerically.The optimization method chosen was a ''Genetic Algorithm'' (GA) with penalty functions for the constraints. Chen and Huang [9], have studied the optimal placement of CLD treatment of plates. The approach chosen is an extension of the approach in Ref. [8] into two dimensions. The optimization method is a combination of what the authors call a ''Topographical method'' and a ''Complex method'', but these methods are not described further neither are there any references to these methods. Genetic optimization technique has also been used for problems with several goal functions, see e.g., Ref. [10]. The technique is referenced to as multi-objective genetic algorithm (MOGA) where in the actual case the ACLD treatment of a beam is being optimized with respect to the weight of the structure, the shape of the beam and the control voltage.

For problems where the goal function is linearly dependent on integer values of the design variables, which can be either zero or one, Balás method (see Ref. [11]) is an efficient method for solving the problem. A potentially large number of searches through possible values of the design variables are reduced to only a small part of the possible number of combinations, and the iteration process will end up with the optimal solution or evidence that there does not exist any feasible solution. The method is also referred to as pseudo-dual simplex method. If the goal function of a nonlinear optimization problem can be expressed as a Taylor series and linearized around a certain value of the design vector, the sequential linear discrete programming method can be used. However, the gradient of the goal function with respect to the design vector has to exist. Similarly, for mixed integer and continuous valued variables, the generalized penalty function method provides a tool for solving the problem, but also requires that the aforesaid gradient exists. In the present study, we aim at solving problems with general boundary conditions and hence the finite-element method (FEM) is chosen as the method of solving for the structural response to the harmonic loading. In this case, we have no difficulties finding and evaluating the goal function. We want to minimize the vibration levels of the plate. A function representative for the frequency-averaged transverse vibration level of the plate is easily found by integrating the "square of the norm" of the vector of nodal transversal velocity amplitudes over the frequency range. By "square of the norm" it is meant the product given by the vector multiplied by its Hermitian transpose. The chosen goal function does not exactly represent the vibrational energy since different nodal velocities might have different phase angles. Instead both "active" and "reactive" energy are included in the expression. But the system is lightly damped, and phase differences from point-to-point are small, and therefore the chosen goal function will be representative for the vibration level. The constraints to the optimization problem are that the ADM material cannot be placed outside the boundaries and that there can only be one coherent piece of ADM material placed onto the base-line structure. The latter condition is resulting from a cost perspective. When it comes to the choice of optimization method we want fast convergence and for that reason a gradient-based optimization method is preferable. But the difficulty is to find the gradient of the goal function with respect to the design variables which are the possible locations of ADM patches. The ADM patches can be added onto the structure as discrete, finite size, pieces at permissible positions. The goal function contains the square of the nodal transverse velocity amplitudes, which in turn are calculated by the inversion of the dynamic stiffness matrix of the problem. Inside the dynamic stiffness matrix, we find our design variables. For this type of plate problems, no analytical expression for this gradient has been found. The conclusion is that we have to seek for a hybrid approach where for each iteration, each possible location for ADM placement is investigated in terms of the gradient of the goal function under the constraint that an ADM patch can only be placed in a certain pattern that is industrially feasible. Although the extensive literature outlining research within the field of optimization, no such method has been found. The work outlined below aims at presenting a solution to the problem.

2. Problem description

A plate subjected to a transverse harmonic vibration at its sides is considered. The vibration of the boundaries is uniform and synchronous, i.e., the amplitude is constant along the sides and all points along the boundaries are vibrating in-phase. The remaining degrees of freedom along the sides of the plate are locked. A typical cross-section of the plate and the principles of the loading and boundary conditions are shown in

Fig. 1. Problem definition showing a flat plate with a synchronous vibration of the boundary. The boundary of the plate are fixed in all directions except the direction of the vibration.

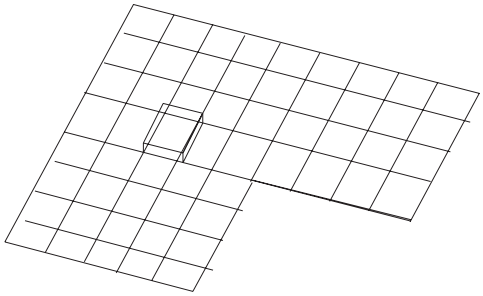

Fig. 2. Principle for how ADM pieces can be added onto existing FE structure. Note that the ADM piece has to have the same shape as the existing underlying element.

Fig. 1. The plate is flat but there is no limitation in shape or size. The frequency range of the imposed vibrations is relatively broad, typically 100–5000 Hz. The problem is supposed to simulate a typical panel in an automobile application where several local deformation modes will occur over a relatively broad frequency range of excitation. The plate is modelled by means of the FEM using shell elements. It is supposed that the ADM material can be added to the structure in pieces coinciding with the surface area of each element, see Fig. 2. The problem is then to find the optimal number and placement of such ADM pieces with respect to the desired reduction in average surface velocity of the base line structure. The optimization problem is then formulated as

$$\mathrm{Min}[J(\mathbf{x})] \tag{1}$$

under the constraint

$$\mathbf{x} = \mathbf{x}_{\mathrm{permissible}}, \tag{2}$$

where J is the goal function and $\mathbf{x}_{\mathrm{permissible}}$ is the vector of permissible positions (or elements) for placement of ADM onto the existing structure.

3. Goal function

For a plane wave, the radiated sound pressure is proportional to the surface velocity in the normal direction of the radiating surface. The corresponding expression for the acoustical energy contains the square of the pressure level. Even if a lower vibration level not necessarily results in a lower sound radiation for all frequencies, over all, lower vibration levels are key in order to reduce the radiated sound, see e.g., Ref. [12]. implies that an essential term in the definition of a suitable goal function is the square of the surface velocity. Let us denote this value v_S and we conclude that given a vector $\mathbf{v}$ of nodal transverse complex velocity amplitudes from a finite-element solution, we easily find this value from

$$v_{\mathrm{S}} = (\mathbf{v}^{\mathrm{H}}\mathbf{v}), \tag{3}$$

where index H denotes the Hermitian transpose. But $\mathbf{v} = \mathbf{v}(f)$ so in order to get an averaged effect over the whole frequency range, we therefore define the goal function J as

$$J = \int_{f=f_{\min}}^{f_{\max}} \mathbf{v}(f)^{\mathrm{H}}\mathbf{v}(f)\mathrm{d}f, \tag{4}$$

where $\mathbf{v}(f)$ is the vector of complex nodal velocity amplitudes in the transverse direction at the actual frequency. The calculation of the integrand in the frequency domain is naturally done at discrete frequency steps and hence the integral in Eq. (4) is approximated and replaced by a sum as (assuming equidistant

frequency steps)

$$J_a = \sum_j \mathbf{v}(f_j)^H \mathbf{v}(f_j). \tag{5}$$

The unit for our chosen goal function is hence m^2/s^2. It shall be pointed out that for evaluating the effect of ADM treatment, the analysis is preferably done in terms of a comparison between a "base-line" structure and the same structure with ADM added on. Therefore, the frequency spacing when using Eq. (5) must be the same in the two cases to be compared.

4. Permissible positions for ADM patches

In this study, ADM material is supposed to be added to the base line structure piece by piece in a mosaique manner. The ADM pieces of material can have a shape that is exactly the same as the actual finite-element of the base-line structure to which it is supposed to be attached, see again, Fig. 2.

In the first iteration, all elements in the base-line model represent permissible positions. But in forthcoming iterations, new ADM pieces can only be added so as to create a coherent pattern. The reason for this is that, practically, in industrial applications it would be too expensive to deal with several pieces. Therefore, an index system is created, where it is kept track on row and column numbers for each position. Permissible indices relative to a chosen position with index (i,j) are therefore

$$(\text{row},\ \text{column}) = (i,j-1),(i,j+1),(i-1,j) \quad \text{or } (i+1,j)$$

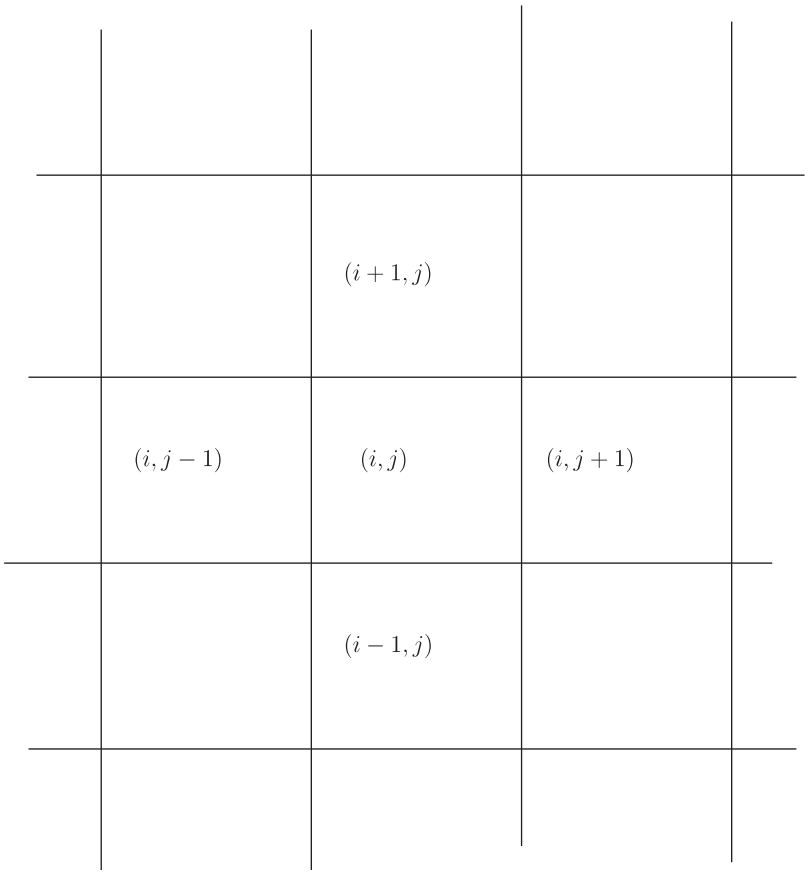

Fig. 3. Row and column indices for the elements in the finite-element model of the base-line structure.

as shown in Fig. 3, provided that any of the four options above are not already chosen as an ADM patch position or that any of the four options above would result in a position not existing in the base-line structure.

5. Solution procedure

We seek the optimal use of ADM material placed onto an existing structure (“base-line structure”) that is subject to boundary vibrations. The independent variable of the problem is therefore the possible positions where ADM can be added. In principle, we are looking for the numerical estimate of gradient of the goal function with respect to the independent parameter, which is the vector of permissible positions. An analytical expression for this gradient has not been found. Instead, we have to calculate the value of the goal function for each of the permissible positions in each iteration, and then determine which position that is the most favorable to use for placement of ADM. The solution flow chart is shown in Fig. 4. First, a base-line FE model is built, representing the original problem. The base-line problem is solved, resulting in the base-line nodal velocity amplitudes. Then, a number of administrative matrices are set up, in order to keep track on the solution parameters. We are then ready to start the iterations, where the first action in each iteration is to determine which positions that are permissible for ADM. Then, the highest gradient in terms of position is identified, and ADM is hence placed in this position. In this study, different “stop conditions” can be used. Here, the following stop conditions are implemented:

- the gradient of the goal function is becoming positive, i.e., more ADM pieces would increase the goal function instead of decreasing it,
- the maximum cost that we want to spend in terms of ADM material cost is reached,

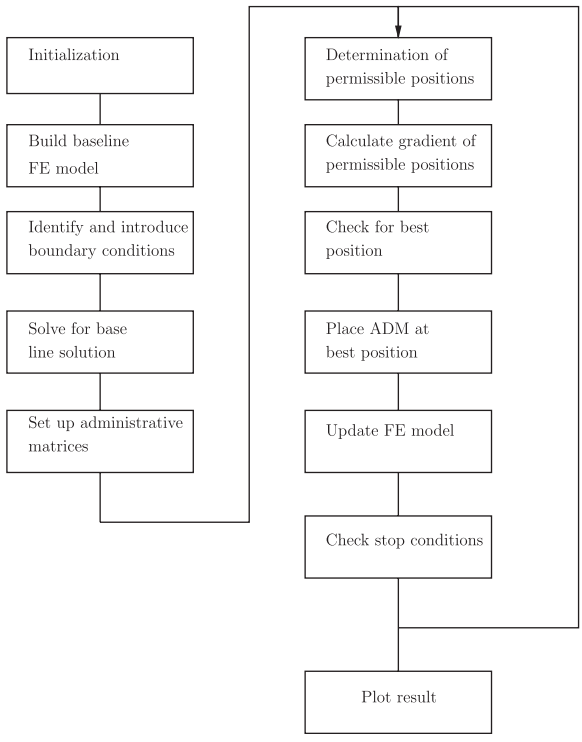

Fig. 4. Solution procedure to the optimization problem.

- the maximum weight allowed for the treatment is reached or
- the maximum area of the available surface that we can use is reached.

Finally, the value of the goal function is plotted against iteration number.

6. FE modelling

In this study, an in-house FE code has been used. The code has been implemented in MATLAB. The base-line structure is modelled using membrane and plate elements in combination, so as to simulate a shell element. The ADM is modelled in the same way as in Ref. [1], i.e., the cover layers are modelled using shell elements while the viscoelastic layer is modelled using a special interface element that couples the two cover layers together. A linear interpolation procedure is used in the in-plane directions of this interface element. There are 5 degrees-of-freedom for each node, and we hence get in total 40 degrees-of-freedom for the ADM "patch". For more details regarding the FE modelling, see Ref. [1]. During the optimization procedure, the ADM patches are added onto the existing FE model at chosen positions. The structural FE matrices must be able to increase and decrease in size when more degrees-of-freedom are added to the problem. In terms of the actual FE modelling of the structure, a simplification is made in that for double-sided constraining layer ADM patches, the ADM patch lower level nodes share locations with the base-line structure, see Fig. 5. A more correct way of coupling the ADM patch FE structure to the base-line structure, would have been to offset the ADM patch node locations from the base-line structure and then define the correct coupling between the ADM patch lower level nodes and the base-line structure nodes, but since we are primarily interested in the optimal position and use of the ADM material this modelling imperfection was not considered to have any influence on the result of the optimization. For single-sided constraining layer ADM patches though, the constraining layer is connected to the base-line structure via the interface element in a standard way, and there is no such approximation involved as mentioned above.

7. Numerical results and discussion

7.1. Square aluminum plate

A fictitious example with a square aluminum plate with side length 150 mm is investigated. The thickness of the plate is 1.0 mm. The modulus of elasticity for the aluminum material is set to 71 GPa and the Poisson ratio is set to 0.29. A numerical damping factor has been introduced by multiplying the stiffness matrix of the base-line structure with the factor $(1 + 0.015\mathrm{i})$ in order to make the frequency–response curves smooth and thereby to minimize the risk of missing out a peak completely or to hit a peak perfectly, which would mislead the optimization procedure. The eigenfrequencies of the plate are given in Table 1. Here, the ADM material is a three layer steel–rubber–steel sandwich material, see Fig. 6. The thickness of the steel layers is 0.5 mm and the thickness of the viscoelastic layer is 0.1 mm. The modulus of elasticity for the steel material is set to 206 GPa and the Poisson ratio is set to 0.30. The rubber material is modelled in the same way as in Ref. [1]. Hence, in the frequency range of 100–2000 Hz, the real part of the complex shear modulus varies from approximately 10–41 MPa and the loss factor varies from 0.79–0.99. Also from Ref. [1], the Poisson number is set to 0.4993. The densities are 2800, 7707 and 1300 $\mathrm{kg/m^3}$ for the aluminum, steel and rubber materials, respectively. The

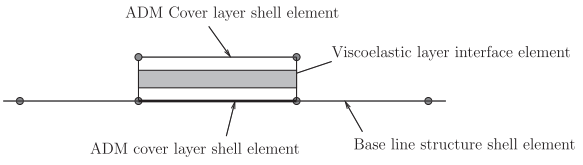

Fig. 5. Finite-element modelling of the attachment of the ADM piece onto the base-line structure.

Table 1
Calculated eigenfrequencies for square plate

Mode	1	2	3	4
Frequency (Hz)	390.3	795.7	1173	1426

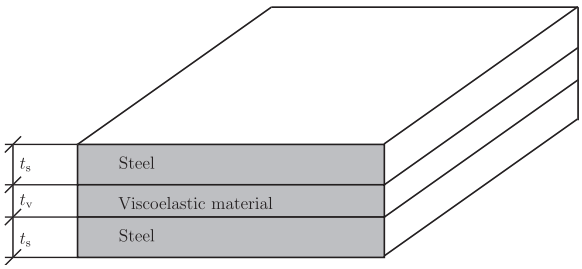

Fig. 6. Layer configuration of the ADM material. In the picture, the thickness of the viscoelastic layer is exaggerated. The thickness of the steel layers is 0.5 mm and the thickness of the viscoelastic layer is 0.1 mm.

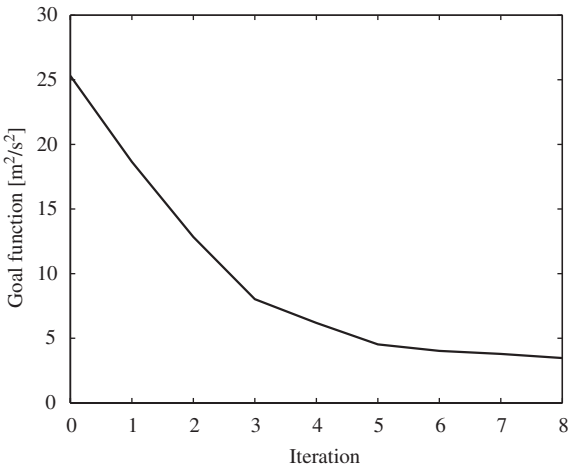

Fig. 7. Goal function versus iteration number for a frequency range covering the first eigenfrequency.

base-line finite-element mesh consists of 6×6 elements. In the first run, we optimize the use of ADM towards the first eigenmode and choose the frequency range to the interval 200–400 Hz. In this case, all nodes at the boundaries of the plate were excited with a prescribed transverse harmonic displacement with an amplitude of 0.01 m. All other degrees of freedom at the boundaries were locked. The result of the optimization is shown in Fig. 7. The start value of the goal function is 25.3 m^2/s^2 and the end value after 9 iterations is 3.47m^2/s^2. This corresponds to a decrease of the goal function with 8.6 dB. The order in which the ADM patches are placed is shown in Fig. 8. After 9 iterations, the gradient of the goal function switched sign and became positive and the corresponding stop condition came into force. Since the first eigenmode does not exhibit any nodal lines, the largest strains are in the middle of the structure, and hence the optimal place to add ADM is where the displacement amplitude is the largest. The transverse displacement amplitude at the evaluation point (see Fig. 8)is shown in Fig. 9. Results are presented for base-line structure (without ADM) and for the plate with ADM after the last iteration. It is interesting to see how the peak response is shifted towards lower frequencies

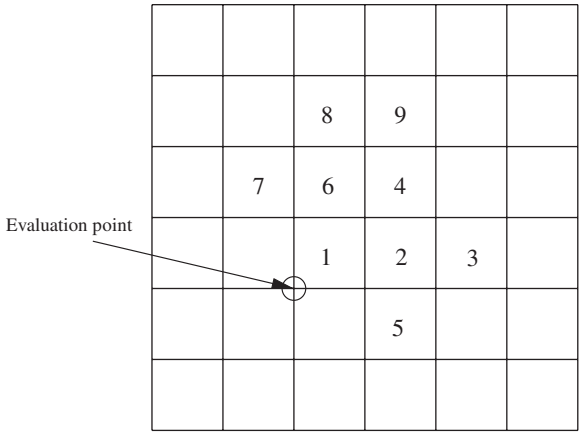

Fig. 8. Optimal positions of ADM pieces on the square aluminum plate for each iteration in the optimization run. Frequency range covering first eigenfrequency. Evaluation point for the frequency response function is shown.

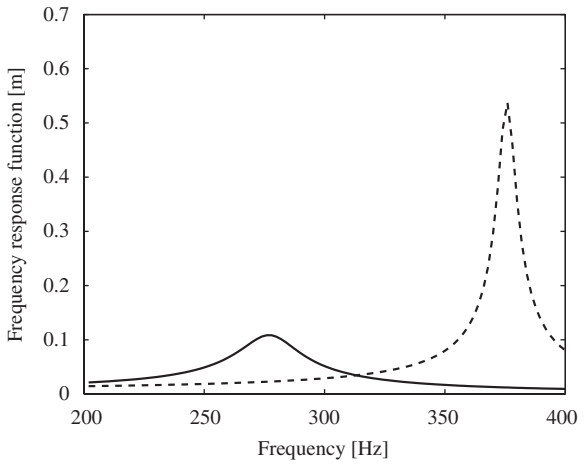

Fig. 9. Transverse displacement amplitude versus frequency at the evaluation point of the aluminum square plate. Dashed line represents base-line structure while solid line represents plate with attached ADM after last iteration. Frequency range covers the first eigenfrequency.

after that the ADM pieces have been added. At the same time, the displacement amplitude has been significantly decreased.

If we instead choose to optimize towards the second eigenmode, we cover the frequency range 600–800 Hz. In this case, we cannot excite the plate via a uniform, synchronous vibration of the boundaries since the generalized force of this antisymmetric mode is zero because of a perfect symmetry of the loading. Instead, we apply a unit harmonic point load of 1.0 N in a node offset from the nodal lines for the modes of interest, and keep all boundaries clamped. The corresponding development of the goal function is shown in Fig. 10 and the patch placement order together with the load input point and the evaluation point are shown in Fig. 11. In this case, the parameters for the stop conditions were set to correspond to 10 iterations for the element size given and after 10 iterations, the optimization loop stopped. The impression is that ADM is mainly placed along one diagonal of the plate. The explanation to this might be that the load drives a local deformation mode with high displacements along one diagonal. The start value of the goal function is $1.02 \times 10^{-6}\,\mathrm{m^2/s^2}$ and the end value is $1.48 \times 10^{-8}\,\mathrm{m^2/s^2}$, so the reduction in goal function this time is 18.3 dB. The corresponding displacement amplitude is shown in Fig. 12.

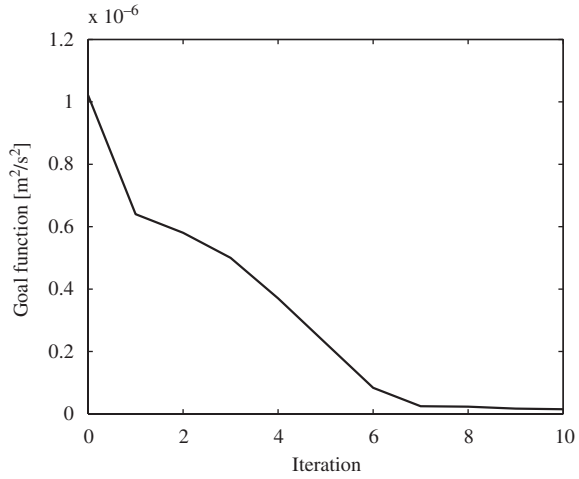

Fig. 10. Goal function versus iteration number for a frequency range covering the second eigenfrequency.

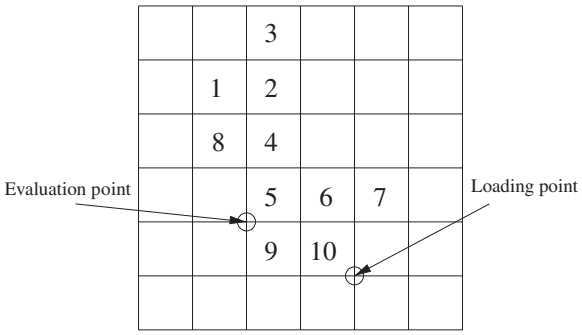

Fig. 11. Optimal positions of ADM pieces on the square aluminum plate for each iteration in the optimization run. Frequency range covering second eigenfrequency. Evaluation point and loading point are shown.

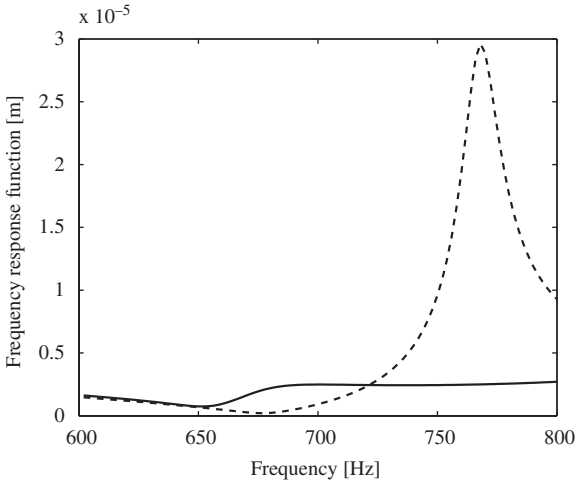

Fig. 12. Transverse displacement amplitude versus frequency at the evaluation point of the aluminum square plate. Dashed line represents base-line structure while solid line represents plate with attached ADM after last iteration. Frequency range covers the second eigenfrequency.

7.2. Industrial example

An industrial and realistic example in terms of a square plate with a nonsymmetric cut out is studied. The side length of the plate is 180 mm and the thickness of the plate is 4 mm. The dimensions are typical for a panel from an oil pan or a front cover of the engine of a car. Also, the thickness of the plate is chosen to give the first four eigenfrequencies in the range of 2000–4000 Hz, which is typical for automotive applications. The plate is made of the same Aluminum material as in the foregoing example. The ADM material used in this study is different from the type in the example above, but the constitutive model material parameters for the rubber are the same. This material is single-sided with respect to the constraining layer. The ADM material consists of a 0.5 mm thick steel material and a 0.2-mm-thick rubber layer. The rubber side of the ADM material is vulcanized directly onto the base-line structure.

7.2.1. Experimental set up

The plate is mounted in a relatively stiff fixture, see Fig. 13. The purpose of the fixture is to be stiff enough in the transversal direction in order to provide a synchronous transversal vibration of the boundary of the plate, via a point load from a shaker which is applied to the fixture. Also, the attachment of the plate to the fixture shall be stiff enough in order to prevent rotations of the plate about the in-plane directions. As can be seen from the pictures for the first three eigenmodes (Figs. 14–16), this is almost the case. There is only a relatively limited rotation of the plate at the boundary to the fixture. Thus, the corresponding boundary condition in an FE analysis should impose zero displacements and rotations in all directions except for the transversal direction which is prescribed. The excitation of the fixture is done using an electromagnetic shaker of the type "Wilcoxon F4/F7" with a built in force gage sn 9943. The response amplitude is measured by a laser equipment of the type "Polytec PSV 300 scanning laser vibrometer" including software version 8.22.

7.2.2. FE studies

In parallel, FE studies were made of the same plate. In these studies, 20 3D solid elements with a reduced integration formula were used in the in-plane directions. The finite-elements were square in shape and the side length of the elements was 9 mm. The same mesh density was later used in the optimization runs in order to produce comparable results. For a comparison, a more dense finite-element mesh was studied. Here, 25 times more elements were used compared to the coarse mesh of the same type as above. In Table 2 a comparison is made between the eigenfrequencies from the measurement and the eigenfrequencies from the two FE runs. The calculated eigenfrequencies for the coarse mesh is about 10 percent higher than the corresponding

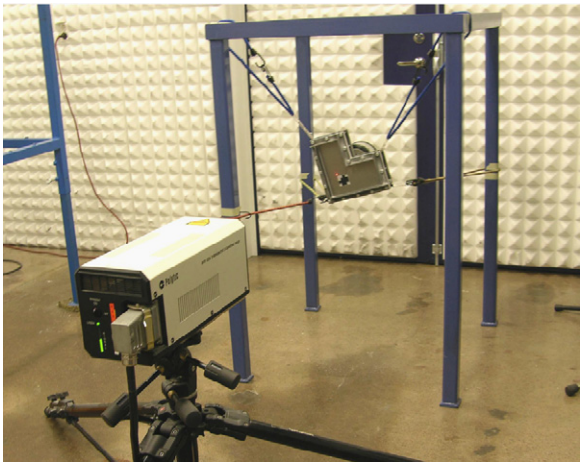

Fig. 13. Experimental set up.

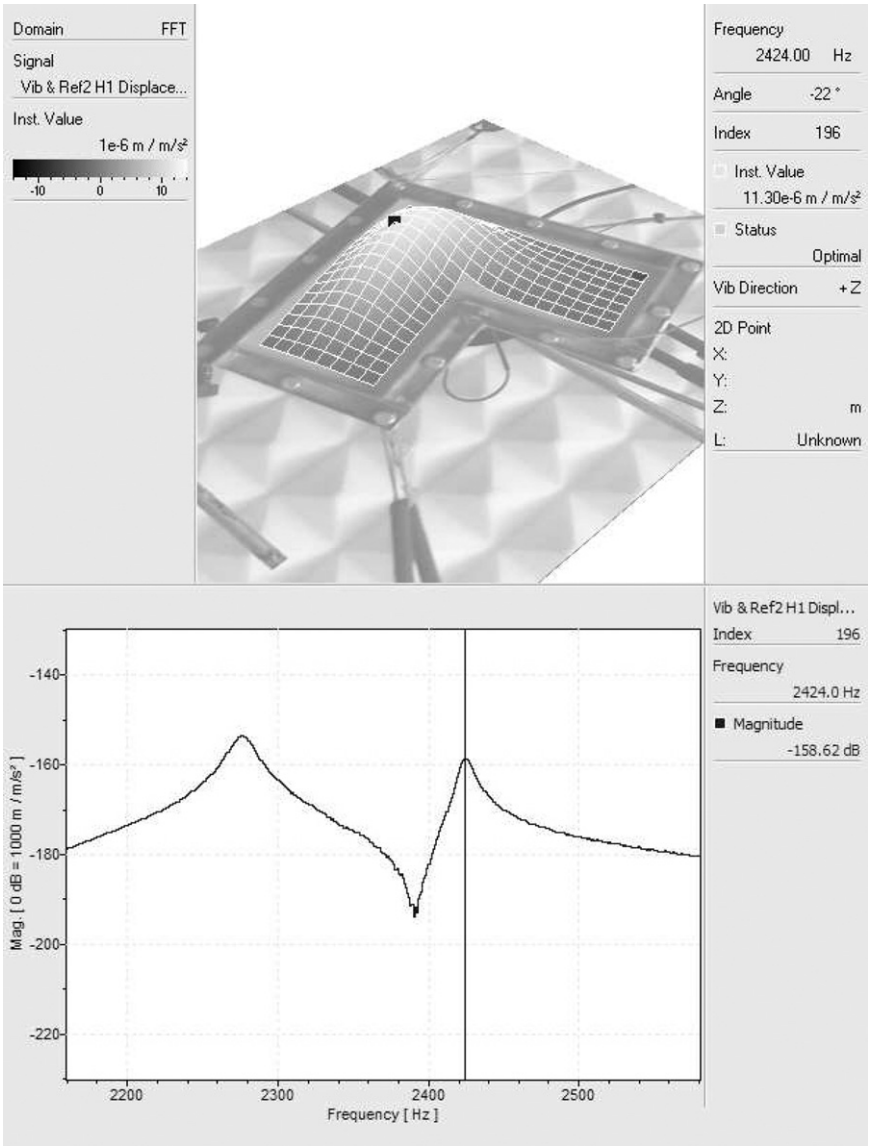

Fig. 14. Upper: measured isolines for first eigenmode. Lower: measured transfer function between fixture reference acceleration and surface displacement at point indicated by the black square in upper figure. Note that the first peak represents a fixture mode.

measured eigenfrequencies. It is expected that a relatively coarse FE mesh results in higher stiffness compared to a measurement and furthermore, in reality, the rotational stiffness of the fixture is not infinite and hence the effective dimensions of the plate is larger which results in lower eigenfrequencies. However, a comparison between measurements and calculations of the decrease of the vibration level of the plate after applying ADM, will still be relevant.

7.2.3. Optimization

The optimization procedure outlined above is applied also to this problem. The chosen frequency interval is 2500–4000 Hz, covering the first three eigenfrequencies. Since we have a lower limit in terms of the resolution in the frequency domain and since a completely undamped system would result in infinitely high-response levels at the eigenfrequencies, results could be inaccurate if a numerical damping is not introduced. The introduced damping will make the frequency response curves become more smooth, and hence, we will not

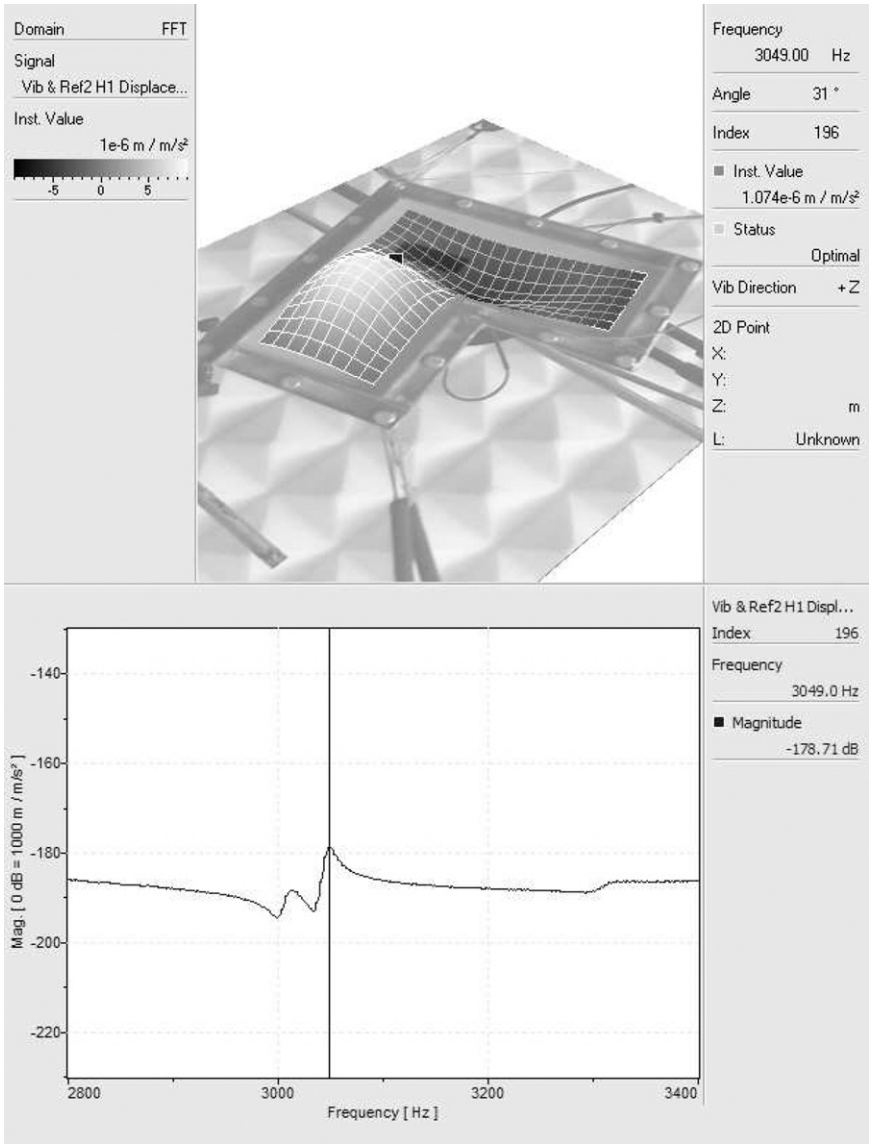

Fig. 15. Upper: measured isolines for second eigenmode. Lower: measured transfer function between fixture reference acceleration and surface displacement at point indicated by the black square in upper figure.

face the risk of missing out a peak or hit a peak perfectly which would make the optimization code draw the wrong conclusions on where to optimally place the ADM material. By inspecting the result from the measurements, described below, a numerical damping was introduced by multiplying the stiffness matrix with the factor $(1 + 0.0036i)$. Also, in order to save computer time, the frequency interval for the calculation of the goal function was split up into three shorter intervals:

- 2500–2685 Hz covering the first eigenmode using 92 frequency steps,
- 3250–3350 Hz covering the second eigenmode using 50 frequency steps and
- 3835–3915 Hz covering the third eigenmode using 40 frequency steps.

Thus there were about 2 Hz resolution around all three eigenfrequencies under consideration, in order to get comparable results. The development of the goal function as function of iteration number is shown in Fig. 17.

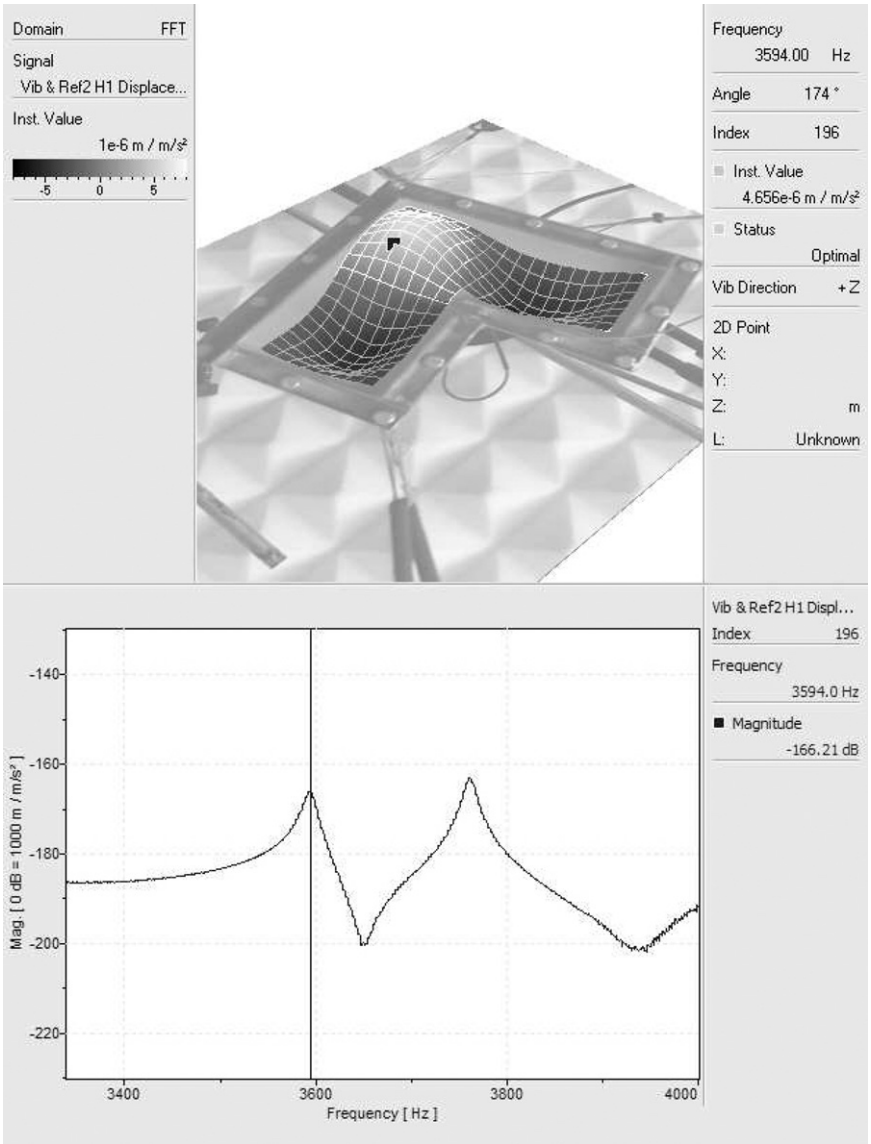

Fig. 16. Upper: measured isolines for third eigenmode. Lower: measured transfer function between fixture reference acceleration and surface displacement at point indicated by the black square in upper figure. Note that the second peak represents a fixture mode.

Table 2
Measured and calculated eigenfrequencies for industrial example

Mode	Measured freq (Hz)	FE freq, coarse (Hz)	FE freq, fine (Hz)
1	2424	2661	2609
2	3049	3351	3296
3	3594	3973	3908
4	4746	4927	4863

Also here, the maximum number of iterations allowed was set to 10. The average decrease in vibration level over the frequency range of interest was calculated to be approximately 1.7 dB. However, the decrease for individual modes was higher, up to 3–4 dB, see Table 3. An average decrease of 1.7 dB might seem

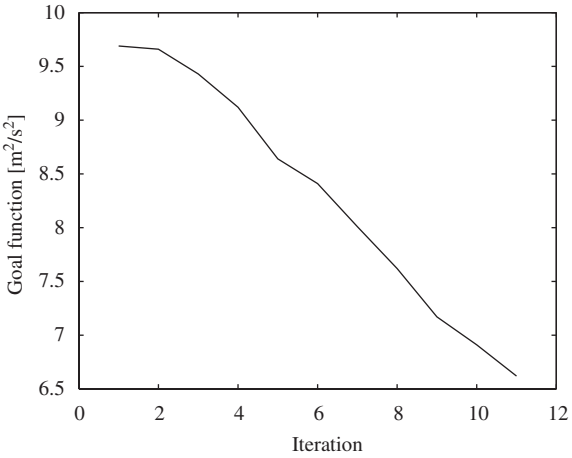

Fig. 17. Goal function versus iteration number for a frequency range covering the first three eigenmodes. Industrial example.

Table 3
Measured and calculated reduction of vibration level after application of ADM

Mode	Measured reduction (dB)	Calculated reduction (dB)
1	3.2	3.0
2	−0.15	−3.0
3	4.0	1.9

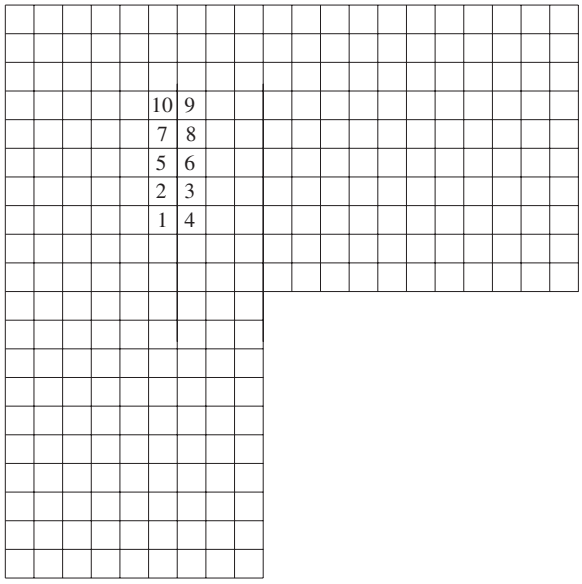

Fig. 18. Optimal positions of ADM pieces for each iteration for a frequency range covering the first three eigenfrequencies. Industrial example.

modest, but should be viewed in relation to the small surface that is covered with ADM after 10 iterations. The order of the placement of ADM pieces onto the base-line structure as a result of the optimization is shown in Fig. 18.

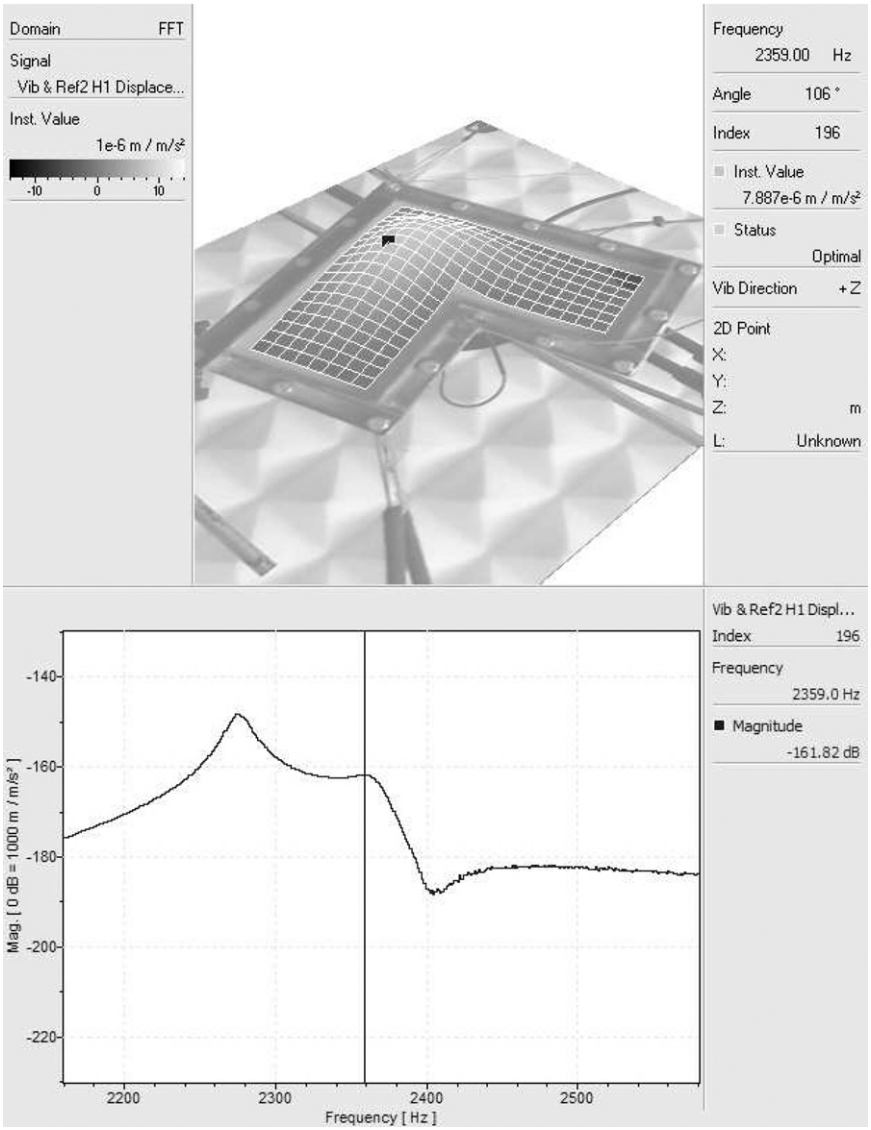

Fig. 19. Upper: measured isolines for first eigenmode for plate with optimized position of ADM. Lower: measured transfer function between fixture reference acceleration and surface displacement at point indicated by the black square in upper figure. Note that the first peak represents a fixture mode. Industrial example.

7.2.4. *Reference measurements*

The corresponding pattern of ADM as shown in Fig. 18 was then mounted on the plate (as one piece of material). Measurements of the vibration levels were then performed over the three eigenfrequencies in the range from 2500–4000 Hz. The result was then extracted for the same frequency range as in the optimization procedure. The results from the measurements with ADM mounted on the base-line structure are shown in Figs. 19–22. The coherence curves of the measurements are shown in Fig. 22 and it can be seen that the coherence is reasonably good. It should be noted that a number of "fixture modes" are also excited besides the "plate modes" for different frequencies and the plate modes therefore have to be identified manually in order to make the comparisons. A comparison with the calculated result in terms of the reduction values as a result of the application of ADM is shown in Table 3. It is clear that the optimisation procedure has identified that

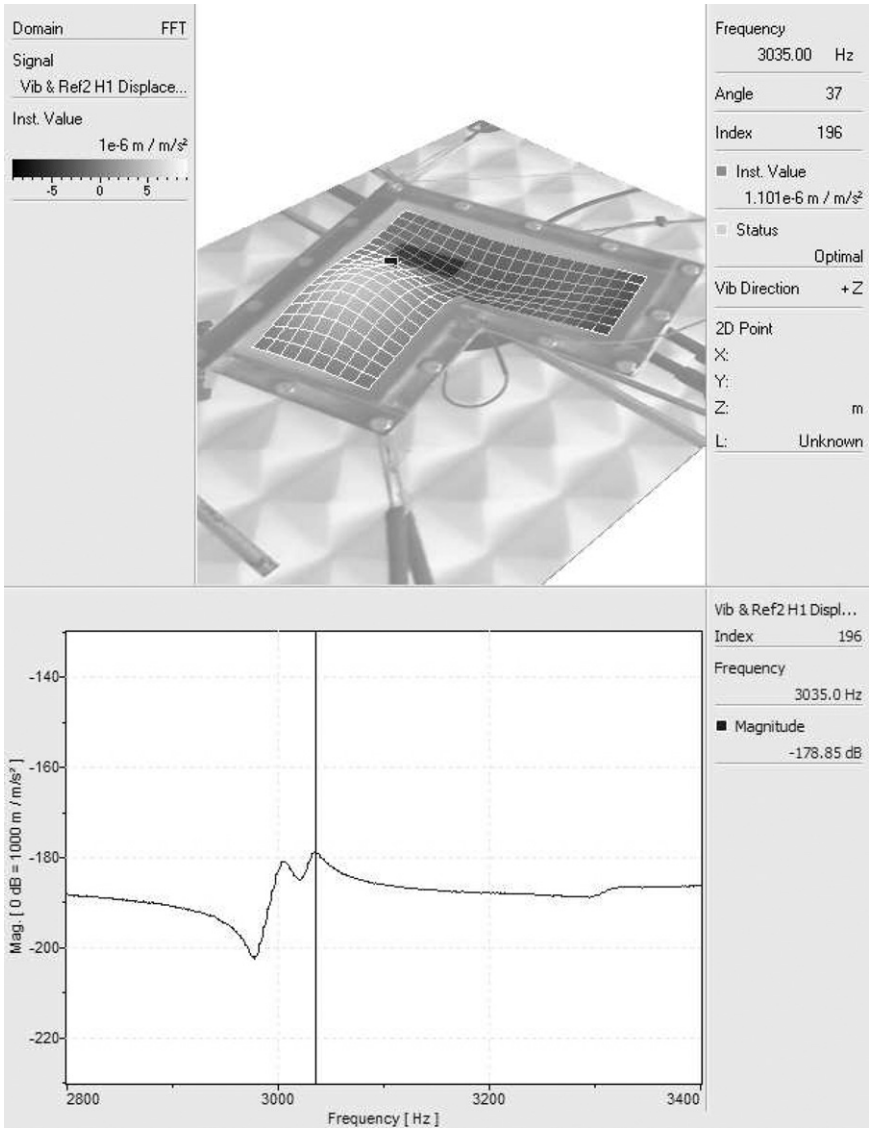

Fig. 20. Upper: measured isolines for second eigenmode for plate with optimized position of ADM. Lower: measured transfer function between fixture reference acceleration and surface displacement at point indicated by the black square in upper figure. Industrial example.

reduction of the vibration levels for Modes 1 and 3 would give best benefit for a certain amount of ADM material to spend, and hence, the ADM piece is placed where Modes 1 and 3 have the highest displacements.

The conclusion is that the agreement for the first mode is excellent. The agreement for the second mode is not in line with the result for the first mode but this mode has a much lower vibration amplitude, in fact more than 15 dB lower than the first mode, and comparisons are therefore much more uncertain. The third mode has about 8 dB lower vibration amplitude compared to the first mode. Given the complexity of the problem where we do have a certain degree of interaction with fixture modes in the measurement, the agreement for the third mode is acceptable. The outcome of the optimization procedure therefore seems reasonable and the ADM has been placed in order to create a positive impact on the dominant vibration modes (the first and the third).

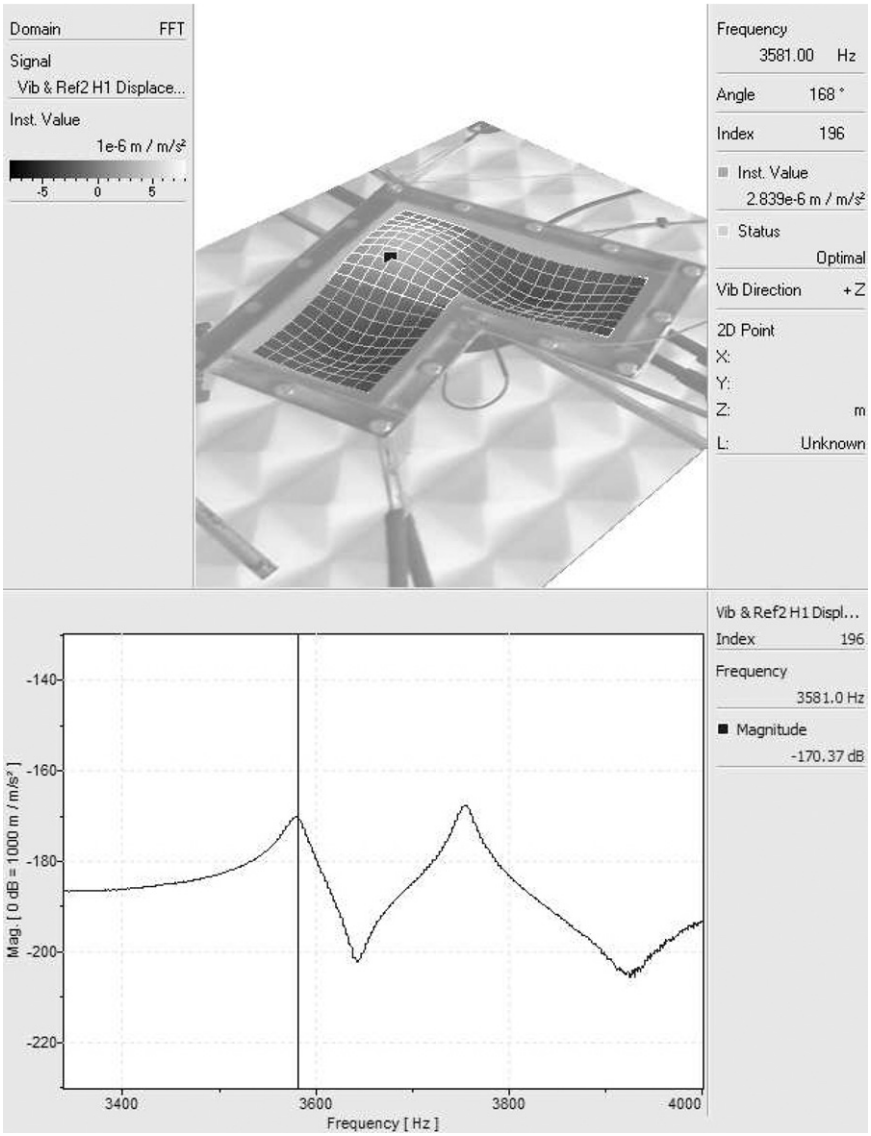

Fig. 21. Upper: measured isolines for third eigenmode for plate with optimized position of ADM. Lower: measured transfer function between fixture reference acceleration and surface displacement at point indicated by the black square in upper figure. Note that the second peak represents a fixture mode. Industrial example.

8. Conclusions

A design method for optimal positioning of attached constrained damping layers is developed and its purpose is demonstrated by examples. The result of the method is compared with measurements of specimens of industrial relevance. Based on these comparisons, it can be concluded that the method is stable and efficient. The optimization routine involved is of gradient type, resulting in a reasonable rate of convergence. It has been shown in a study of a simple square plate that for lower order modes, the vibration level can be reduced by up to 18 dB by covering less than 30 percent of the surface with ADM. In an industrial example, the average vibration level for a representative panel in automotive engine applications was decreased by approximately 1.7 dB by the placement of a piece of ADM representing about 3.4 percent of the surface. The corresponding decrease of the vibration levels for the dominant modes were 3–4 dB.

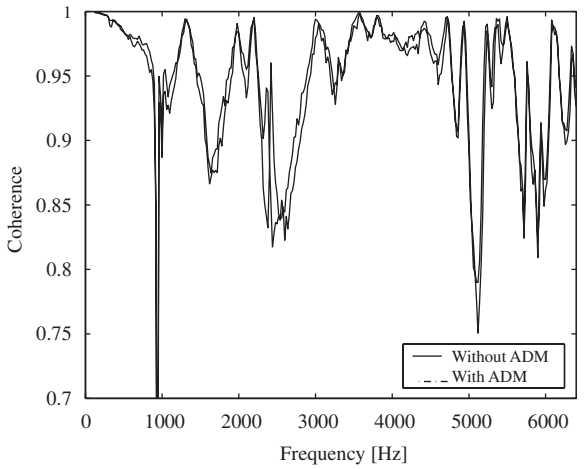

Fig. 22. Coherence for measurements with and without ADM.

Acknowledgments

Pontus Paulsson at Trelleborg Rubore AB did all the measurements.

References

[1] M. Alvelid, M. Enelund, Modelling of constrained thin rubber layer with emphasis on damping, *Journal of Sound and Vibration* 300 (2007) 662–675.
[2] P.A. Nelson, S.J. Elliott, *Active Control of Sound*, Academic Press, New York, 1992.
[3] M. Alvelid, Optimisation of secondary sources for active noise control in a FE-model of an aircraft cabin, *Proceedings of Inter Noise* 93 (1) (1993) 65–70.
[4] O.R. Tutty, P. Hackenberg, P.A. Nelson, Gradient-based control and optimization of boundary layer transition, *Proceedings of the Institution of Mechanical Engineers* 214 (2000) 347–359.
[5] K.H. Back, S.J. Elliott, Natural algorithms for choosing source locations in active control systems, *Journal of Sound and Vibration* 186 (1995) 245–267.
[6] M. Moshrefi-Torbati, A.J. Keane, S.J. Elliott, M.J. Brennan, E. Rogers, Passive vibration control of a satellite boom structure by geometric optimization using genetic algorithm, *Journal of Sound and Vibration* 267 (2003) 879–892.
[7] Y. Liu, K.W. Wang, Damping optimization by integrating enhanced active constrained layer and active-passive hybrid constrained layer treatments, *Journal of Sound and Vibration* 255 (2002) 763–775.
[8] H. Zheng, C. Cai, X.M. Tan, Optimization of partial constrained layer damping treatment for vibrational energy minimization of vibrating beams, *Journal of Mechanical Sciences* 44 (2002) 1801–1821.
[9] Y. Chen, S. Huang, An optimal placement of cld treatment for vibration suppression of plates, *Journal of Mechanical Sciences* 44 (2002) 1801–1821.
[10] L.C. Hau, E.H.K. Fung, Multi-objective optimization of an active constrained layer damping treatment for shape control of flexible beams, *Smart Materials and Structures* 13 (2004) 896–906.
[11] S.S. Rao, *Engineering Optimization*, Wiley, New York, 1996.
[12] L. Kari, K. Lindgren, F. Leping, A. Nilsson, Constrained polymer layers to reduce noise: reality of fiction?—an experimental inquiry into their effectiveness, *Polymer Testing* 21 (2002) 949–958.